Variance Gamma process in the option pricing model

Jakub Drahokoupil

FFA Working Paper 2/2021

FACULTY OF FINANCE AND ACCOUNTING

Bibliographic information:

Drahokoupil, J. (2021). *Variance Gamma process in the option pricing model*. FFA Working Paper 2/2021, FFA, Prague University of Economics and Business, Prague.

This paper can be downloaded at: wp.ffu.vse.cz

Contact e-mail: ffawp@vse.cz

Variance Gamma process in the option pricing model

Author

Jakub Drahokoupil[1]

Abstract

The aim of this paper is to apply Variance Gamma process in the option pricing model and compare it with the well-known and widely used option pricing model, the Black-Scholes model. The Variance Gamma model is, in contrast to the one-parameter Black-Scholes model, a three-parameter model. In addition, these two parameters, which are included in the Variance Gamma model, serve to model the skewness and kurtosis of the empirical distribution of the logarithmic returns of the underlying asset. An important part of this work is also a comparison of suitable valuation algorithms for calculation of the option price using the Variance Gamma model. The comparison of both models will be performed primarily on historical empirical distributions of logarithmic returns of selected stocks. Then, performance and pricing error of both models will be tested when estimating implied coefficients based on market data of the options. The performance of both models will be measured by traditional statistical-econometric methods such as RMSE, Likelihood ratio, Akaike information criterion and last but not least by the Natural spline regression model, which estimates the effect of the variable "Moneyness" (distance between the strike price and the current asset value) on the pricing error. All tests performed in this work suggest that the Variance Gamma model is a more accurate model for calculating the price of options.

AMS/JEL classification: G13, C10

Keywords: option pricing models; Variance Gamma model; Lévy processes; Black-Scholes model; Fast Fourier Transformation; Stochastic processes

1. Introduction

One of the most used models for option pricing, Black-Scholes model, relies on several significant assumptions, of which some have been with certainty proven to be not valid in the real world. Existence of non-Gaussian character of the logarithmic returns or the stochastic volatility are examples proving invalidity of certain Black-Scholes model assumptions. Other Black-Scholes model's assumptions, such as infinite variance of the underlying stochastic process (price of the underlying asset may not rise to infinity) or the assumption of almost surely continuous trajectories of the underlying process (existence of jumps), are practically unrealistic (CONT R., Empirical properties of asset returns: stylized facts and statistical issues, 2002).

[1] Jakub Drahokoupil; Department of Banking and Insurance, Faculty of Finance and Accounting, Prague University of Economics and Business, Prague, Czech Republic; Email: draj05@vse.cz.

This paper has been prepared under the financial support of the Czech Science Foundation Grant research project 18-05244S, "Innovation Approaches to Credit Risk Management", and by the VŠE internal grants IGA 102029 and IP100040/1020.

Several authors have already addressed the problematics of Non-Gaussian characters, for example Mandelbrot or Fama, even before the publication of Black-Scholes model. Gaussian character of the empirical distribution may be violated in the three dimensions. First, the kurtosis of the empirical distribution may be higher (and in most cases truly is) or lower. Second the skewness may be non-zero, or the empirical distribution will have so called Fat Tails (TALEB, 2013). In fact, regarding the finance world, the empirical distributions are mostly leptokurtic (higher kurtosis and fat tails). The Variance Gamma model (process) is one of the promising models (processes) which may be able to estimate the empirical distribution more accurately and may be able to remove, or at least highly reduce, the volatility smile phenomenon, as it is possible that it may be partially caused by the inaccurate estimation of the risk within the Black-Scholes model framework.

The second main problematics mentioned above, stochastic volatility, can be proofed when the volatility level is plotted with the time on the x-axis and volatility level on the y-axis. There exist periods where volatility is higher and periods where it is low. The level of the volatility often changes suddenly by the jump (SCHOUTENS, 2003) and (BATES, 1996). However, Variance Gamma model does not include the solution for this problematic and will not be discussed any further in this paper.

2. Variance Gamma process and Lévy process

Variance Gamma process, Wiener process or Poisson process are all stochastic processes which belong among the Lévy processes, named after the French mathematician Paul Lévy. The Lévy processes include continuous and jump (point) processes (CAPASSO, 2005). Variance Gamma process is pure jump process without any continuous component. However, it is a process that accounts for high activity by having an infinite number of jumps in any interval of time, by which it may resemble the Brownian motion. Thus, Variance Gamma process could more accurately describe the empirical leptokurtic financial distributions of logarithmic returns, as price development of the asset is often influenced by the suddenly incoming and highly important price-making information, which results rather in the significant price jump. Models, which include jumps, then offer better matematical apparatus for higher and less often price jump, which implies the Fat Tail leptocurtic ditributions. (FIORANI, 2009). We can define the general Lévy process with the following definitoin:

Definition: Lévy process
Let φ(u) be characteristic function of the distribution. If, for each positive natural number n, is the function φ(u) also n^{th} power of the very same characteristic function φ(u), then the distribution is infinitely divisible.

For each such infinitely divisible distribution we may define the stochastic process $X = \{X_t, t \geq 0\}$.
The X *can be called Lévy process when the following is applicable:*

- *X origins in zero*
- *X has independent and stationary increments such that its distribution over* $[s, s+t]$ *where* $s, t \geq 0$, *or* $X_{t+s} - X_s$ *has characteristic function equal to* $\left(\varphi(u)\right)^t$
- *The process fulfils the càdlàg property, or its trajectories* $\{X_t\}$ *are continuous from right and there exist a limit from the left*
- *For any* $\varepsilon > 0$ *is* $\lim_{s \to 0} \mathrm{P}(|\mathrm{X_{t+s}} - \mathrm{X_t}| > \varepsilon) = 0$

(SCHOUTENS, 2003)

2.1. Variance Gamma process

In the previous chapter, it has been shown that the approximation of the empirical logarithmic returns with the Non-Gaussian process may lead to more accurate description of the future price behaviour and thus may lead to more accurate estimation of the option price. It has been shown that the appropriate alternative process may come from the family of the Lévy processes. The Variance Gamma process from this family of stochastic processes may be the appropriate one and its application will be discussed further in the paper.

The Variance Gamma process can be constructed throughout two definitions. For better understanding of this process, both definitions will be now presented.

1st definition of Variance Gamma process – with the Brownian component

Let's assume stochastic process $G = \{G_t; t \geq 0\}$ *as subordinating gamma process with parameters* μ *as mean rate and* ν *as variance rate. Next, let's assume stochastic process* $W = \{W_t; t \geq 0\}$ *as an independent standard Brownian motion. Stochastic process* $V = \{V_t; t \geq 0\}$ *can be called Variance Gamma process, if for* $\theta \in \mathrm{R}$ a $\sigma > 0$ *the following is applicable*

$$V_t = \theta G_t + \sigma W_{G_t} \qquad \textbf{1}$$

And its characteristic function is defined in terms of Brownian motion W_t *and gamma process* G_t *with unit mean rate,* $\mu = 1$*, as*

$$\Phi V_t(u; \sigma, \nu, \theta) = \left(1 - iu\nu\theta + \frac{1}{2}\sigma^2 u^2 \nu\right)^{-\frac{t}{\nu}} \qquad \textbf{2}$$

We can state that the Variance Gamma process begins in the zero, has stationary and independent increments, which are randomly sampled from the three parametric Variance Gamma distribution $\mathrm{VG}(\sigma, \nu, \theta)$. These parameters represent:

(i) σ - volatility of the Brownian motion

(ii) ν - variance of time shift, which is define by the subordinating gamma process

(iii) θ - drift of Brownian motion

The kurtosis of the process is modelled by the parameter ν, skewness by the parameter θ (MADAN, CARR, & CHANG, 1998(2)).

2nd definition of Variance Gamma process – without Brownian component

Let the Lévy measure of Variance Gamma process be

$$\upsilon VG(dx) = \begin{cases} C\ exp(Gx)|x|^{-1}\ dx & x < 0 \\ C\ exp(-Mx)x^{-1}\ dx & x > 0 \end{cases} \quad \textbf{3}$$

where

$$C = t/\nu > 0$$

$$G = \left(\sqrt{\frac{1}{4}\theta^2\nu^2 + \frac{1}{2}\sigma^2\nu^2} - \frac{1}{2}\theta\nu\right)^{-1} > 0 \quad \textbf{4}$$

$$M = \left(\sqrt{\frac{1}{4}\theta^2\nu^2 + \frac{1}{2}\sigma^2\nu^2} + \frac{1}{2}\theta\nu\right)^{-1} > 0$$

Variance Gamma process can be then constructed as

$$V_t = G_t^1 - G_t^2 \quad \textbf{5}$$

Where for gamma process G_t^1 *for* $t \geq 0$ *are its parameters* $\mu = C$ *and* $\nu = M$*, for the gamma process* G_t^2 *for* $t \geq 0$ *are its parameters* $\mu = C$ and $\nu = G$ (FIORANI, 2009), (APPLEBAUM, 2004).

The characteristic function of the process under the second definition is

$$\Phi V_t(u;\ C, G, M) = \left(\frac{GM}{GM + (M - G)iu + u^2}\right)^C \quad \textbf{6}$$

Variance Gamma proess has, on the finite interval, infinetely many jumps, though its trajectories have finite variance. Even though both definitions are relatively different, when the characteristic function from the 2nd definition is transformed and its parameters C, G and M are substituted with their respective equations, the same characteristic function of the process, as presented in the 1st definition, can be obtained. Then, it is proved that the Variance Gamma process can be constructed by both definitions

$$1)\ \Phi V_t(u;\ C, G, M) = \frac{GM}{GM}\left(\frac{1}{1 + \left(\frac{1}{G} - \frac{1}{M}\right)iu + \frac{u^2}{GM}}\right)^C \quad \textbf{7}$$

$$2)\ \Phi V_t(u;\ C, G, M) = \left(1 + \left(\frac{1}{G} - \frac{1}{M}\right)iu + \frac{1}{GM}u^2\right)^{-C}$$

3) $\Phi V_t(u;\ C, G, M)$

$$= \left(1 + \left(\left(\sqrt{\frac{1}{4}\theta^2\nu^2 + \frac{1}{2}\sigma^2\nu^2} - \frac{1}{2}\theta\nu\right) - \left(\sqrt{\frac{1}{4}\theta^2\nu^2 + \frac{1}{2}\sigma^2\nu^2} + \frac{1}{2}\theta\nu\right)\right)iu \right.$$
$$\left. + \left(\sqrt{\frac{1}{4}\theta^2\nu^2 + \frac{1}{2}\sigma^2\nu^2} - \frac{1}{2}\theta\nu\right)\left(\sqrt{\frac{1}{4}\theta^2\nu^2 + \frac{1}{2}\sigma^2\nu^2} + \frac{1}{2}\theta\nu\right)u^2\right)^{-1/\nu}$$

4) $\Phi V_t(u;\ C, G, M) = \left(1 + (-\theta\nu)iu + \frac{1}{2}\sigma^2u^2\nu\right)^{-t/\nu}$

In the following tables, the moments for both symmetric and non-symmetric Variance Gamma distribution based on 1st and 2nd definition. The moments are defined for the time of length equal to 1.

Table 1: Variance Gamma distribution – 1st definition

Parameter	$V(\sigma, \nu, \theta)$	$V(\sigma, \nu, 0)$
E(X)	θ	0
Variance	$\sigma^2 + \nu\,\theta^2$	σ^2
Skewness	$\nu\theta\,(3\sigma^2 + 2\nu\theta^2)/(\sigma^2 + \nu\,\theta^2)^{3/2}$	0
Kurtosis	$3(1 + 2v - v\sigma^4\,(\sigma^2 + \nu\,\theta^2)^{-2})$	$3(1 + v)$

Data source (SCHOUTENS, 2003)

Table 2: Variance Gamma distribution – 2nd definition

Parameter	$V(C, G, M)$	$V(C, G, G)$
E(X)	$C(G - M)/(MG)$	0
Variance	$C(G^2 + M^2)/(MG)^2$	$2CG^{-2}$
Skewness	$2C^{-1/2}(G^3 - M^3)/(G^2 + M^2)^{3/2}$	0
Kurtosis	$3(1 + 2C^{-1}(G^4 + M^4)/\,(G^2 + M^2)^2)$	$3(1 + C^{-1})$

Data source (SCHOUTENS, 2003)

Based on the parameters from the first definition, we can deduce following attribute of the Variance Gamma distribution. If we do not consider only one-time interval, we can write the kurtosis as

$$3\left(1 + \frac{v}{t}\right) \qquad \textbf{8}$$

Furthermore, we can conclude, that with the rising *t*, the kurtosis will converge to the value of three, which is typical for the normal distribution. We can expect that the phenomenon of the higher kurtosis

and probably the fat tails will be the most significant for the high frequency and daily log-returns, whilst the long-term log-returns will converge to the normal distribution.

2.2. Variance Gamma process and option pricing

Dynamics of the price of the underlying asset may be modelled, using the Variance Gamma process, by replacing the Geometric Brownian motion process in the Black-Scholes model equation with the Variance Gamma process equation. So, we can write the following equation:

$$S(t) = S(0)\exp\left(mt + X\left(t;\sigma_p,\nu_p,\ \theta_p\right) + \omega_p t\right)$$
$$dP_t\ = P_t\left(e^{r_f dt}\ - 1\right) \qquad \textbf{9}$$

Where $X(\,.\,)$ is the Variance Gamma process, m is the expected value of the returns of the underlying asset (mostly the stock) given by the probability measure P, which is also indicated by the coefficient p at each variable. The variable ω constitutes a "correction factor" excluding the possibility of arbitrage. The variable ω can be derived from a characteristic function of Variance Gamma distribution mentioned above with the $u = \frac{1}{i}$, where we get

$$E[S(t)] =\ S(0)\exp(mt) \Leftrightarrow E\left[\exp\left(X(t)\right)\right] = \exp(-\omega_s t) \qquad \textbf{10}$$

and from the (KONIKOV & MADAN, 2002)

$$\omega_s = \frac{1}{\nu} ln\left(1 - \nu\theta - \frac{1}{2}\sigma^2\nu\right) \qquad \textbf{11}$$

3. Comparison of Variance Gamma model solutions

In order to price the call option with the Variance Gamma model, we must be able to get the solution of the equation

$$C(S(0),K,t) = \exp(-rt)\,E(\max[S(t) - K, 0]) \qquad \textbf{12}$$

where $S(t)$ is defined in the equation 9 from the previous section. In the following paragraphs, several possible approaches, how to price call option with the Variance Gamma model will be presented.

3.1. Numerical solution of Variance Gamma PIDE

Variance Gamma (VG) Partial Integro-Differential Equation (PIDE) describes the option price dynamics when the underlying returns are described by a Variance Gamma process. The VG PIDE can be solved by the commonly used numerical solution, Finite difference method. The VG PIDE will be solved by the IMEX scheme proposed by the (CONT & VOLTCHKOVA, A Finite Difference Scheme for Option Pricing in Jump Diffusion and Exponential Lévy Models, 2005). Firstly, it is neccesary to derive the PIDE of the Variance Gamma model, (CONT & VOLTCHKOVA, Integro-differential equations for option prices in

exponential Lévy models, 2005) deduce and prove that the option pricing PIDEs in the Lévy models are so-called „viscosity solutions[2]“ of the general valuation PIDE

$$\frac{\partial V(t,x)}{\partial t} - rV(t,x) + \left(r - \frac{1}{2}\sigma^2 - \int_R (e^z - 1 - z)\nu(dz)\right)\frac{\partial V(t,x)}{\partial x} + \frac{1}{2}\sigma^2\frac{\partial^2 V(t,x)}{\partial x^2} + \int_R \left(V(t,x+z)\nu - V(t,x) - z\frac{\partial V(t,x)}{\partial x}\right)\nu(dz) = 0 \quad \textbf{13}$$

With the following boundary conditions for call option

$$\begin{aligned} V(t,x) &= \max(e^x - K, 0) \\ V(t,x) &\overset{(x \to -\infty)}{=} 0 \\ V(t,x) &\overset{(x \to \infty)}{\sim} e^x - Ke^{-r(T-t)} \end{aligned} \quad \textbf{14}$$

And for put option

$$\begin{aligned} V(t,x) &= max\ (K\ - e^x, 0) \\ V(t,x) &\overset{(x \to \infty)}{=} 0 \\ V(t,x) &\overset{(x \to -\infty)}{=} Ke^{-r(T-t)} \end{aligned} \quad \textbf{15}$$

For the VG model we can get the PIDE in the following form

$$\frac{\partial V(t,x)}{\partial t} + \left(r - \frac{1}{2}\sigma_\varepsilon^2 - \omega_e\right)\frac{\partial V(t,x)}{\partial x} + \frac{1}{2}\sigma^2\frac{\partial^2 V(t,x)}{\partial x^2} + \int_{|z|\geq\varepsilon} V(t,x+z)\nu(dz) = (\lambda_\varepsilon + r)V(t,x) \quad \textbf{16}$$

Where

$$\begin{aligned} \sigma_\varepsilon^2 &:= \int_{|z|\geq\varepsilon} z^2\nu(dz) \\ &\int_{|z|\geq\varepsilon} (e^z - 1)\nu(dz) \\ \lambda_\varepsilon &:= \int_{|z|\geq\varepsilon} \nu(dz) \end{aligned} \quad \textbf{17}$$

[2] For more detailed information see for example (KATZOURAKIS, 2014)

And Lévy measure is equal to

$$\nu(dz) = \frac{e^{\frac{\theta z}{\sigma^2}}}{\kappa|z|}\exp\left(-\frac{\sqrt{\frac{2}{\kappa}+\frac{\theta^2}{\sigma^2}}}{\sigma}|z|\right)dz \qquad \textbf{18}$$

From the (CONT & VOLTCHKOVA, A Finite Difference Scheme for Option Pricing in Jump Diffusion and Exponential Lévy Models, 2005) we use the IMEX scheme described in the following paragraph, where the differential part of the equation will be solved with the implicit method and integral part of the equation with the explicit method. With the explicit method for the integral part, we are not forced to calculate the inverse matrix to so called „Jump matrix" described further in the text. Integral part of the scheme can be also calculated with the Fast Fourier Transformation discribed further as well.

The Variance Gamma process has infinite activity, which means that if the step size converges to an infinitesimal value, then conversely the number of new jumps will converge to infinity $\lambda := \int_{-\infty}^{\infty}\nu(z) = \infty$. It is necessary to exclude the interval $-\varepsilon < z < \varepsilon$, which will result in the finiteness of the above-mentioned parameters. Furthermore, for any $0 < K_1 < K_2$ we select values $\boldsymbol{B_1}$ and $\boldsymbol{B_2}$ such, that it is ensured

$$[-B_1, B_2] = \left[\left(-K_1 - \frac{1}{2}\right)\Delta x, \left(K_2 + \frac{1}{2}\right)\Delta x\right] \qquad \textbf{19}$$

Where we are interested in this linear space $[0,T] \times [A_1 - B_1, A_2 + B_2]$.

The next step is to discretize the integral from the PIDE equation

$$\int_{-B_1}^{B_2} V(t, x+z)\nu(dz) \approx \sum_{k=-K_1}^{K_2} v_k V_{i+k}^n \qquad \textbf{20}$$

where

$$v_k = \sum_{\left(k-\frac{1}{2}\right)\Delta x}^{\left(k+\frac{1}{2}\right)\Delta x} \nu(dz), \qquad pro\ -K_1 < k < K_2 \qquad \textbf{21}$$

Let $\hat{\lambda} = \sum_{k=-K_1}^{K_2} v_k$, then for high values of $\boldsymbol{B_1}$and $\boldsymbol{B_2}$, parameter λ is appropriate approximation of λ, because the following applies

$$\lambda = \lim_{B_1, B_2 \to \infty} \hat{\lambda} = \lim_{B_1, B_2 \to \infty} \sum_{B_1}^{B_2} \nu(dz) \qquad \textbf{22}$$

And the final discretization of VG PIDE with the IMEX scheme is

$$\frac{V_i^{n+1} - V_i^n}{\Delta t} + \left(r - \frac{1}{2}\sigma_\varepsilon^2 - \omega_e\right)\frac{V_{i+1}^n - V_{i-1}^n}{2\Delta x} + \frac{1}{2}\sigma^2\frac{V_{i+1}^n + V_{i-1}^n - 2V_i^n}{\Delta x^2} - (\lambda_\varepsilon + r)V_i^n + \sum_{k=-K_1}^{K_2} v_k V_{i+k}^{n+1} = 0 \quad \textbf{23}$$

Rearranged as

$$\overbrace{V_i^{n+1} + \Delta t \sum_{k=-K_1}^{K_2} v_k V_{i+k}^{n+1}}^{\widetilde{V_i^{n+1}}} = V_i^n\left(1 + (\hat{\lambda} + r)\Delta t + \frac{\sigma^2\Delta t}{\Delta x^2}\right) + V_{i+1}^n\left(-\left(r - \frac{1}{2}\sigma^2 - \hat{\omega}\right)\frac{\Delta t}{2\Delta x} + \frac{1}{2}\frac{\sigma^2\Delta t}{\Delta x^2}\right) + V_{i-1}^n\left(\left(r - \frac{1}{2}\sigma^2 - \hat{\omega}\right)\frac{\Delta t}{2\Delta x} + \frac{1}{2}\frac{\sigma^2\Delta t}{\Delta x^2}\right) \quad \textbf{24}$$

And when the brackets are further parametrized then

$$\widetilde{V_i^{n+1}} = aV_i^n + bV_{i+1}^n + cV_{i-1}^n \quad \textbf{25}$$

Finally, we can solve the system V_i^n for $\forall\, i\ 1 \le i \le M-1$

a) With the jump matrix as

$$\begin{cases} \widetilde{V_i^{n+1}} = V_{i+1}^n + \Delta t\, \mathcal{J}\, V^{n+1} \\ V^n = \mathcal{D}^{-1}\left(\widetilde{V_i^{n+1}} - B\right) \end{cases} \quad for\ \forall\, i\ 1 \le i \le M-1 \quad \textbf{26}$$

With $\mathcal{J}$ being a jump matrix with the Lévy measure vector beginning in the all elements on the main diagonal

With example of Lévy measure

$$\begin{pmatrix} 7.29 \cdot 10 - 4 \\ 0 \\ 0 \\ 0 \\ 3.34 \cdot 10 - 8 \end{pmatrix} \quad \textbf{27}$$

and example of $\mathcal{J}$

$$\begin{pmatrix} 7.29\cdot 10-4 & 0 & 0 & 0 & 3.34\cdot 10-8 & 0 & 0 & 0 & 0 & 0 \\ 0 & 7.29\cdot 10-4 & 0 & 0 & 0 & 3.34\cdot 10-8 & 0 & 0 & 0 & 0 \\ 0 & 0 & 7.29\cdot 10-4 & 0 & 0 & 0 & 3.34\cdot 10-8 & 0 & 0 & 0 \\ 0 & 0 & 0 & 7.29\cdot 10-4 & 0 & 0 & 0 & 3.34\cdot 10-8 & 0 & 0 \\ 0 & 0 & 0 & 0 & 7.29\cdot 10-4 & 0 & 0 & 0 & 3.34\cdot 10-8 & 0 \\ 0 & 0 & 0 & 0 & 0 & 7.29\cdot 10-4 & 0 & 0 & 0 & 3.34\cdot 10-8 \end{pmatrix} \quad \textbf{28}$$

Lévy measure vector is obtained as a solution of the $\int_{x1}^{x2} \nu(dz)$, where $x1$ and $x2$ are divisions of the interval

$$\begin{pmatrix} -\left(\frac{Round_{down}(3*std_{VG})}{\Delta x}+1+0.5\right)\Delta x, \\ \left(\frac{Round_{down}(3*std_{VG})}{\Delta x}+1+0.5\right)\Delta x \end{pmatrix} \quad \textbf{29}$$

With the division size equal to $2*\left(\frac{Round_{down}(3*std_{VG})}{\Delta x}+2\right)$ the inner three values are zero, as we excluded the interval $-\varepsilon < z < \varepsilon$ out of the solution space, in this case $[-\varepsilon,\ \varepsilon] = [-1.5\Delta x\ ,1.5\Delta x]$

b) With the FFT and convolution as

$$\begin{cases} \widetilde{V_l^{n+1}} = V_{i+1}^n + \Delta t \sum_{k=-K_1}^{K_2} v_k V_{i+k}^{n+1} \quad for\ \forall\ i\ 1 \le i \le M-1 \\ V^n = \mathcal{D}^{-1}\left(\widetilde{V_l^{n+1}} - B\right) \end{cases} \quad \textbf{30}$$

with $\mathcal{D}$ being a triangular matrix of coefficient a, b, c with boundary conditions

$$B = (aV_0^n, 0, \dots, 0, cV_M^n) \quad \textbf{31}$$

3.2. Analytical solutions of Variance Gamma equation

The analytical solutions for the Variance Gamma model equation can be found in the papers from (MADAN, CARR, & CHANG, 1998(2)) and from (MILNE & MADAN, 2008). While (MADAN, CARR, & CHANG, 1998(2)) propose that the price of call option can be obtained from the following equation

$$\begin{aligned} C(S(0),K,t) &= S(0)\,\Psi\left[d\sqrt{\frac{1-c_1}{v}}, (\varsigma s+s)\sqrt{\left(\frac{1-c_1}{v}\right)^{-1}}, \frac{t}{v}\right] \\ &+ -K\exp(-rt)\,\Psi\left[d\sqrt{\frac{1-c_2}{v}}, (\varsigma s+s)\sqrt{\left(\frac{1-c_2}{v}\right)^{-1}}, \frac{t}{v}\right] \end{aligned} \quad \textbf{32}$$

Where $\Psi(\alpha, \beta, \gamma)$ is function defined on the basis of Bessel function of second order and degenerated hypergeometric function of two variables which can be obtained as solution of the following integral

$$\Psi(\alpha, \beta, \gamma) = \int_0^{+\infty} N\left(\frac{\alpha}{\sqrt{x}} + \beta\sqrt{x}\right) \frac{x^{\gamma-1}\, e^{-x}}{\Gamma(\gamma)}\, dx \qquad \textbf{33}$$

Solution of the integral and more detailed information about the Bessel functions can be found in (GRADŠTEJN, RYŽIK, & JEFFREY, 2007).

The second solution proposed by (MILNE & MADAN, 2008) can be expressed as

$$\begin{aligned} C(g) &= S(0)\left(1 - \frac{v(\varsigma s + s)^2}{2}\right)^{\frac{t}{v}} \exp\left(\frac{g(\varsigma s + s)^2}{2}\right) * N\left[\frac{d}{\sqrt{g}} + (\varsigma s + s)\sqrt{g}\right] \\ &+ -K\exp(-rt)\left[\left(1 - \frac{v(\varsigma s)^2}{2}\right)^{\frac{t}{v}}\right] \exp\left(\frac{g(\varsigma s)^2}{2}\right) * N\left(\frac{d}{\sqrt{g}} + (\varsigma s)\sqrt{g}\right) \end{aligned} \qquad \textbf{34}$$

where $N(\,.\,)$ is cumulative distribution function of the normal distribution and variables d, ς and s are defined as

$$\begin{aligned} \varsigma &= -\frac{\theta}{\sigma^2} \\ s &= \frac{\sigma}{\sqrt{1 + \frac{\left(\frac{\theta}{\sigma}\right)^2 v}{2}}} \\ d &= \frac{1}{s}\left\{\ln\left[\frac{S(0)}{K}\right] + rt + \frac{t}{v}\ln\left[\frac{1 - c_1}{1 - c_2}\right]\right\} \end{aligned} \qquad \textbf{35}$$

and c_1, c_2 are equal to

$$\begin{aligned} c_1 &= \frac{v(\varsigma s + s)^2}{2} \\ c_2 &= \frac{v(\varsigma s)^2}{2} \end{aligned} \qquad \textbf{36}$$

Price of the put option can be obtained with the put-call parity principle.

3.3. Monte Carlo simulation

Monte Carlo simulation solution is based on the simulation of high number of the Variance Gamma process trajectories, where the increments are originating from the three parametric Variance Gamma

distribution. The algorithm in the R Studio software was constructed according to the following scheme:

i. Define input parameters S, K, N, r, T, θ, ν and σ
where S denotes the price of the asset, K strike price of the asset, N is the number of simulated trajectories, r is the interest rate used for the discounting, T is the time and θ, ν and σ are the parameters of Variance Gamma distribution.

ii. Calculate auxiliary variables ϱ a w, G and Norm as

$$\varrho = \frac{1}{\nu}$$

$$w = -\frac{\log\left(1 - \theta * \nu - \frac{\nu}{2} * \sigma^2\right)}{\nu},$$

$$G \sim N * \frac{N * RandGammaDist(shape = \varrho * T)}{\varrho}$$

$$Norm \sim N * RandNormDist(0, 1)$$

Where $N * RandNormDist$ and $N * RandGammaDist$ are vectors of N randomly sampled values from Normal and Gamma distributions. Finally, w is martingale correction term.

iii. Calculate VG random vector as

$$VG_{RV} = \theta * G + \sigma * \sqrt{G} * Norm$$

and vector S in time T

$$S_T = S_0 * \exp\left((r - w) * T + VG_{RV}\right)$$

iv. Calculate the final option value as

$$call = \exp(-r * T) * mean(\max(S_T - K, 0))$$
$$put = \exp(-r * T) * mean(\max(K - S_T, 0))$$

Source: (FU, JARROW, YEN, ELLIOTT, & ed., 2007)

3.4. Fast Fourier Transform

Fourier Transform is mathematical method, which has wide application across the full spectrum of scientific activity, especially in the mathematics and physics, but in the most recent years also in biology or finance. The basic idea of this method, regarding the calculation of the option price, is that when applied on the probability density function, we get the characteristic function. With the Inverse Fourier Transform, we can perform a reverse operation and from the characteristic function obtain a probability density function.

Fourier and Inverse Fourier Transform can be written as

$$S(v) = \int_{-\infty}^{\infty} s(t)\, e^{-2\pi i v t} dt \qquad \textbf{37}$$

and

$$\mathcal{F}^{-1}[S(v)] = s(t) \; = \int_{-\infty}^{\infty} S(v)\, e^{2\pi i v t} dv \qquad \textbf{38}$$

The Fourier Transform can take both continuous and discrete forms, where we are specifically interested in the discrete form (MATSUDA, 2004).

Even thought the Fourier Transformation appears to be elegant tool solving wide range of mathematical issues, in practical use, it encounters application limitations. First, we may encounter an integral without the analytical solution. Second, computer algorithms and software often use discrete alternatives of the continuous functions. Both limitations explain why we are interested especially in the Discrete Fourier Transform, which can be written as

$$S(v) = \Delta t \sum_{k=0}^{N-1} s(t_k) e^{-2\pi i v t_k} \qquad \textbf{39}$$

where $t_k = k\Delta t$ (SCHMELZLE, 2010).

In order to substitute integral with sum, we can use widely known Newton-Cotes equations, specifically the Simpson method.

In general, the computational complexity of the discrete Fourier Transform with the direct methods is $\mathcal{O}(N^2)$, which could cause this method would not be reasonable to use in the practical application. However, we can use so called Fast Fourier Transform family of algorithms, specifically Cooley–Tukey algorithm. This algorithm is based on the paradigm of "Divide and Conquer", where we can lower the computational complexity from $\mathcal{O}(N^2)$ to $\mathcal{O}(N\, logN)$, which speed up the calculation enormously (MALKIN, 2019) (BEKELE, 2016). For detailed description of the algorithm with mathematical proofs see (OSGOOD, 2007). Price of the call option calculated with the Fast Fourier Transform is then according to the (CARR & MADAN, Option valuation using the fast Fourier transform, 1999) using the Simpson method for numerical integration

$$C_T(k) \approx \frac{exp(-\alpha k_u)}{2\pi} \sum_{j=1}^{N} e^{-i\frac{2\pi}{N}(u-1)(j-1)} e^{ibv_j} \psi_T(v_j) \frac{\eta}{3}\left[3 + (-1)^j - \delta_{j-1}\right] \qquad \textbf{40}$$

where δ_n is Kronecker's delta, which is the function that takes values 1 for $n = 1$ and for any other value is equal to zero.

Regarding the equation ***9*** of the Variance Gamma model

$$S(t) = S(0)\exp\left(mt + X(t; \sigma_p, \nu_p, \theta_p) + \omega_p t\right)$$
$$\omega_s = \frac{1}{\nu} ln\left(1 - \nu\theta - \frac{1}{2}\sigma^2 \nu\right) \qquad \textbf{41}$$

and characteristic function of the Variance Gamma process

$$\Phi V_t(u; \sigma, \nu, \theta) = \left(1 - iu\nu\theta + \frac{1}{2}\sigma^2 u^2 \nu\right)^{-\frac{1}{\nu}} \qquad \textbf{42}$$

We can obtain characteristic function for the Variance Gamma model

$$\psi_T(v_j) = \emptyset(u) = \exp[\ln(S_0) + (r+\omega)T]\left(1 - iuv\theta + \frac{1}{2}\sigma^2 u^2 v\right)^{-\frac{T}{v}}) \qquad 43$$

with which we want to substitute $\psi_T(v_j)$ into the call option equation 40 mentioned above. After the substitution, we are able to calculate the call option price using the Fast Fourier Transform.

3.5. Effectiveness and accuracy of each solution

The previously mentioned solutions were transferred into the algorithms in the R Studio software and effectiveness and accuracy of the solutions were compared. Testing of the individual algorithms was performed on the calculation of the price of the call option for the underlying asset, which price trajectory follows Variance Gamma process with these parameters:

S	100
K	101
r	0,1
T	0,25
θ	-0,1436
v	0,3
σ	0,12136

Other additional parameters necessary specifically for each method are listed in the table below along with the calculated price and time needed for the algorithm to converge.

Table 3: Algorithms comparison

Algorithm	Price of the call option	Price calculation time in seconds	Additional algorithm parameters
PIDE 1 – Convolution	3,466584	6,54	Number of time steps and space steps were set to 1000 for both parameters
PIDE 1 – Jump matrix	3,466584	6,44	Number of time steps and space steps were set to 1000 for both parameters
PIDE 2 – Jump Matrix	3,468454	60,66	Number of time steps and space steps were set to 2000 for both parameters
PIDE 3 – Jump Matrix	3,470914	872,56	Number of time steps and space steps were set to 5000 for both parameters
Analytical solution – Bessel Function	3,28544	0,12	Gauss-Kronrod (G20, K41) method is used for the integral solution
Analytical solution – Normal distribution	3,291678	0,43	Gauss-Kronrod (G20, K41) method is used for the integral solution

Monte Carlo simulation	3,474611	3,36	Number of simulated trajectories – 10 000 000
Fast Fourier Transform	3,474164	0,2	Gauss-Kronrod (G20, K41) method is used for the integral solution

Data source: Own calculations

From the table above we can see that PIDE solution via Finite element method does not provide both accurate and at the same time computationally effective results, as the algorithm converges to the FFT and Monte Carlo results with the increasing steps of the calculation very slowly. Both analytical methods are very fast to calculate but show significantly different result than the other methods. Even after multiple revisions of the code and the mathematical theory, author was not able to get the same solutions with the analytical formulas as with the other methods. As both analytical solutions are based on the similar mathematical theory, contrary to other solutions which fundamentals are different, the analytical solutions were assessed to be less accurate. We can see that the Monte Carlo method and FFT method converge to similar results, which are a little higher than solution of PIDE, which increases with the increased number of steps. It is possible to state that the most precise and computationally efficient method is, according to the expectation, Fast Fourier Transform. Numerical solution of PIDE with convolution should be, according to the theory, faster than the solution with Jump Matrix. However, in the R Studio software, convolution function is not implemented efficiently (cannot handle sparse matrix properly), contrary to Python or Matlab software, where the convolution method is almost ten times faster. Based on the Table 3 results, Fast Fourier Transform will be used for the calculation of the option price further in the paper.

4. Data and methods

For verification of the shape of the empirical probability distributions of the underlying asset's logarithmic returns, historical returns of the selected stocks are used. The stocks were on purpose selected from various industries, so as to avoid possible bias present in a specific industry. As the estimation technique, Maximum Likelihood estimation (MLE) method will be used. Following three optimization methods for the MLE will be used to find the most proper parameters describing the empirical distribution:

- Conjugate gradient method [3]
- Broyden–Fletcher–Goldfarb–Shanno (BFGS) algorithm[4]
- Nelder-Mead algorithm[5]

As in the real-world pricing process, implied volatility is used to price the option rather than the historical one, the implied coefficients for both the BS and VG models will be calculated. The underlying data for the implied coefficients calculation will be the market prices of the options for the selected underlying assets. Each options chain defined as the dataset of options with the same underlying asset and maturity and different strike prices will be divided into training and testing set and afterwards, the performance of both models will be compared. Criteria selected for the comparison of the distributions will be Bayesian Information Criterion, comparison of estimated likelihoods and error rate of the model via RMSE metric on train and test dataset. Another significant phenomenon in option pricing is called volatility smile. In general, implied volatility increases as options become more In-the-money or Out-

[3] More detailed information (SHEWCHUK, 1994)
[4] More detailed information (DAI, 2013)
[5] More detailed information (MATHEWS & KURTIS, 2004)

of-the money. It is not uncommon for the implied volatility of OTM / ITM options to be more than ten times higher than the volatility of an At-the-money option. This issue is generally addressed using models that also model volatility. These are models with stochastic or parametric volatility. However, it is possible that at least part of this effect may be caused by the inappropriate use of the BS model and could be at least partially compensated using the VG model. The elimination of the volatility smile effect will be tested by the estimation of the natural spline regression model, where there will be tested the relationship between the moneyness of the option and the pricing error rate of both models.

5. Results and Discussion

5.1. Historical log return distributions

There were eleven companies selected to avoid possible bias of the results, due to the specificity of one particular industry. The list of the selected companies may be found in the Appendix 1 of this paper. For each company, historical logarithmic returns with daily, weekly, and monthly frequency beginning with 01/2010 and ending with 01/2020 were calculated. Afterwards, with the above-mentioned estimation method and comparison criteria, the selected probability distributions were compared. In order to clearly describe the whole comparison process, the Daimler AG returns analysis will be disassembled in detail. During this analysis, we will try to prove, that the VG distribution fits the empirical one better. Also, we will try to prove, that the kurtosis of the distribution will decrease with the decreasing frequency of the logarithmic returns. The decreasing in the kurtosis is one of the Variance Gamma process property described above.

Analysis of the daily logarithmic returns

Figure 1: Daimler log-returns graph - daily

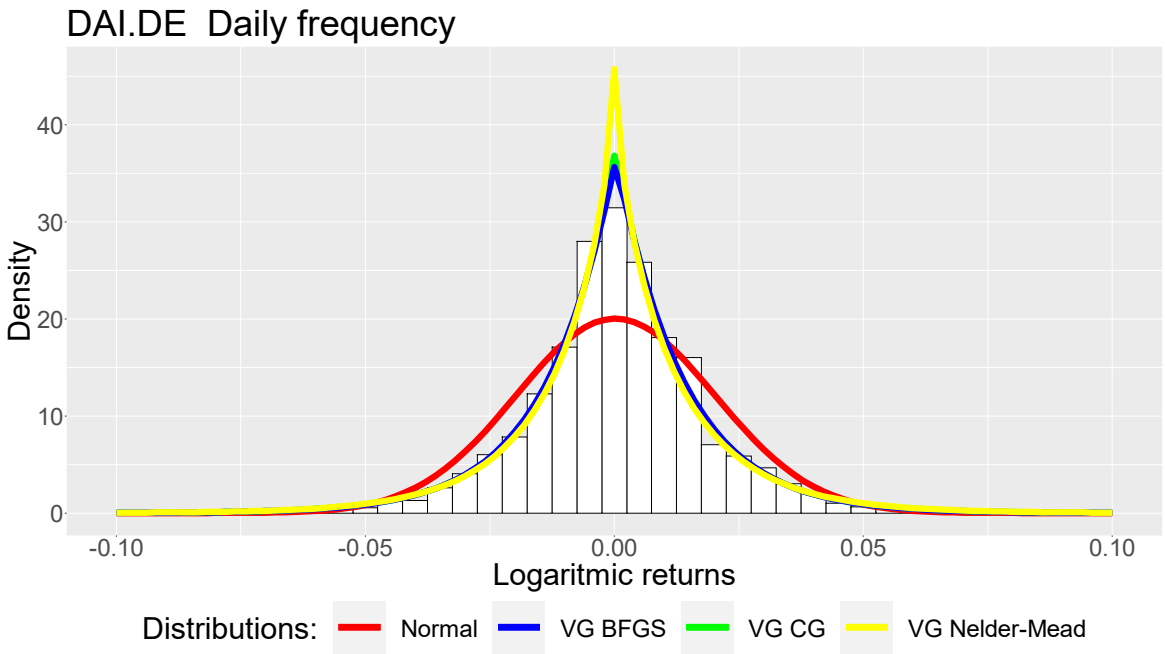

From the Fig. 1 - the graph of the daily logarithmic returns of the Daimler company, it can be clearly seen, that the estimated VG distribution significantly differs from the Normal distribution and that the empirical distribution has higher kurtosis than Normal distribution expects and is able to reflect.

Table 4: Daily historical log-returns statistics

Algorithm	Mean	Sigma	Theta	Kappa	LL	BIC
Normal BFGS	0.000	0.019	NA	NA	6331.797	-12647.92
VG BFGS	0.000	0.019	0.000	0.967	6628.648	-13225.95
VG CG	0.000	0.019	0.000	1.017	6628.317	-13225.28
VG Nelder-Mead	0.000	0.019	0.000	1.229	6621.733	-13212.11

Skewness Empirical	Kurtosis Empirical
-0.049	19.548

Data source: own calculations

If we examine the estimated statistics of the fitted distributions, we can see that VG distribution fitted the empirical one more precisely, measured both by the Log – Likelihood and BIC. We can state that the empirical distribution is neither negatively nor positively skewed, as the Theta of the VG is zero. However, the Kappa is significantly higher than 0, which would VG distribution had, if it matched the Normal distribution (as formula for kurtosis is $3(1+\kappa)$ and normal distribution has kurtosis equal to 3).

Analysis of the weekly logarithmic returns

Fig. 2 shows the same as Fig. 1 with only difference, that there are weekly logarithmic returns. The kurtosis of the empirical distribution is not as different from the normal as in the case of daily log-returns. This matches the theory behind the VG model. Also, the VG distribution seems to be negatively skewed.

Figure 2: Daimler log-returns graph - weekly

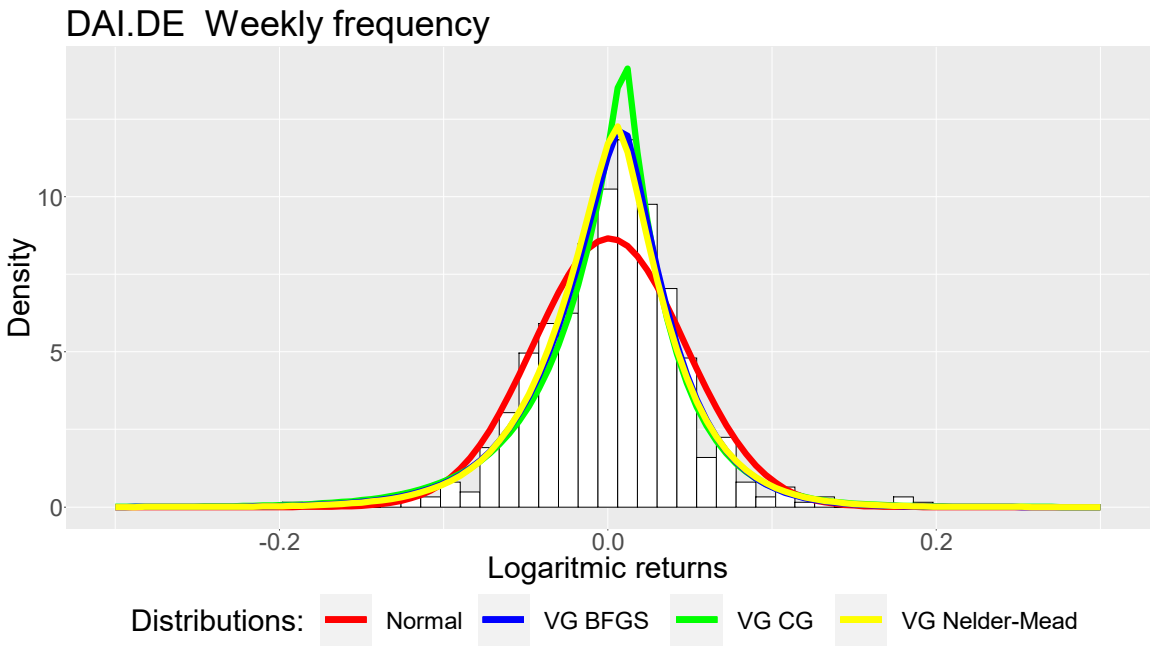

The fitted distribution statistics confirm that the kurtosis is lower than for daily log-returns, but still significantly above the kurtosis of Normal distribution. In this case, the Theta parameter shows the existence of negative skewness. Again, both Log-Likelihood and BIC prefer the VG distribution. Contrary to the previous estimation, for the weekly log-returns, relatively different estimates can be seen for the VG distribution with the above-mentioned algorithms. The reason is that the algorithms had less observations and due to the variant methods behind, the algorithms converged to different coefficient values.

Table 5: Weekly historical log-returns statistics

Algorithm	Mean	Sigma	Theta	Kappa	LL	BIC
Normal BFGS	0.000	0.046	NA	NA	865.613	-1714.08
VG BFGS	0.000	0.045	-0.008	0.678	897.776	-1761.27
VG CG	0.000	0.047	-0.009	1.003	895.352	-1756.42
VG Nelder-Mead	0.000	0.045	-0.005	0.672	897.287	-1760.29

Skewness Empirical	Kurtosis Empirical
-0.435	8.160

Data source: own calculations

Analysis of the monthly logarithmic returns

The last examined logarithmic returns were returns with monthly frequency. The Fig.3 shows that the differences in the optimization algorithms are significant and for example BFGS algorithm may not describe the empirical distribution precisely. Furthermore, the kurtosis is again lower than in the previous cases, proving the decreasing kurtosis assumption.

Figure 3: Daimler log-returns graph - monthly

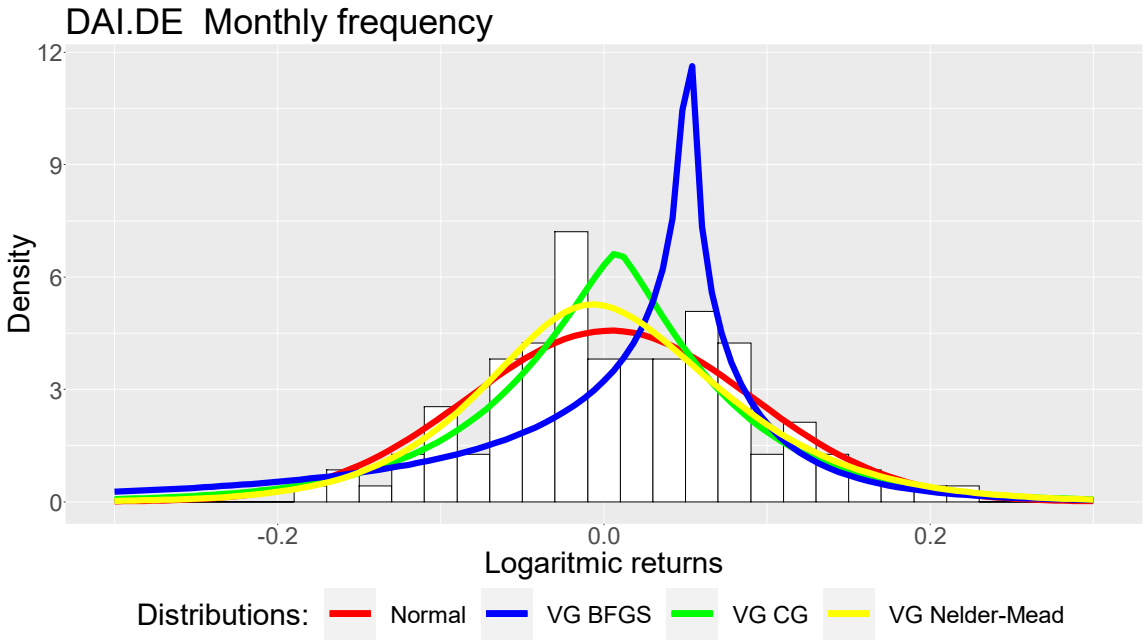

Finally, even though the Log-Likelihood in the Tab. 6 prefers the VG distribution with parameters estimated by the Nelder-Mead algorithm, the BIC prefers the Normal distribution, as the difference between the VG a Normal distribution is not surpassing the BIC penalization for the additional parameters. The Kappa for the Nelder-Mead algorithm is converging to the zero, which indicates the similarity to the Normal distribution.

Table 6: Monthly historical log-returns statistics

Algorithm	Mean	Sigma	Theta	Kappa	LL	BIC
Normal BFGS	0.003	0.087	NA	NA	121.241	-228.28
VG BFGS	0.051	0.107	-0.058	2.085	106.412	-184.43
VG CG	0.008	0.090	-0.005	0.803	122.143	-215.89
VG Nelder-Mead	-0.016	0.086	0.020	0.345	122.727	-217.06

Skewness Empirical	Kurtosis Empirical
-0.530	4.476

Data source: own calculations

Analysis of all datasets

As the single company analysis may bias our results, in the following tables, all the datasets of the historical log-returns are analysed in the same way as the previous Daimler returns.

In Tab. 7 we can see that the Normal distribution is preferred only in two cases measured by the LL and according to the expectations only for the Monthly log-returns.

Table 7: Total historical log-returns statistics – LL

Logarithmic returns	VG	Normal
Total	31	2
Daily	11	x
Weekly	11	x
Monthly	9	2

In Tab. 8 BIC is taken as the decision criteria and filters more historical returns in favour of the Normal distribution. But again, mainly datasets with the lowest frequency.

Table 8: Total historical log-returns statistics – BIC

Logarithmic returns	VG	Normal
Total	27	6
Daily	11	x
Weekly	10	1
Monthly	6	5

Finally, in the Tab. 9 – the average Skewness and Kurtosis of the empirical distributions, calculated as the third and fourth standardized moments, are shown. In average, empirical distributions are slightly negatively skewed, but more importantly have significantly higher Kurtosis with increasing frequency of the log-returns, which indicates fat-tail distribution, where VG distribution prevails over Normal distribution.

Table 9: Total historical log-returns statistics – Skewness and Kurtosis

Logarithmic returns	Skewness	Kurtosis
Daily	-0,32	11,48
Weekly	-0,72	9,64
Monthly	-0,53	5,05

Data source: Yahoo finance

5.2. Implied coefficients estimation

In the previous chapter, historical returns were examined. In reality, implied volatility is used instead of historical one and so the pricing efficiency of both models should be tested on the observed market prices of the listed options.

Implied coefficients were calculated from the options chains with options maturing within a month, six months, and a year. The option prices were obtained as of single snapshot on 22nd October 2020. For each option chain, where options differ by the Strike price and have identical underlying asset and maturity, single vector of implied coefficients was estimated for the VG model as well as single implied volatility was estimated for the BS model. The calibration of the implied coefficients for both models was done via minimizing the Root Mean Square Error (RMSE) metric

$$\min\left(\sqrt{\sum_{i=1}^{N}\frac{C_i^{model}-C_i^{market}}{N}}\right) \qquad 44$$

where N is the number of options in the selected options chain and C is the price of the call option. The BFGS algorithm described above was used for the optimization. Calculation of model price C_i^{model} is done with the FFT algorithm for the VG model. Price C_i^{model} within the BS model was obtained via the well-known formula

$$C = S_t N(d_1) - Ke^{-rt}N(d_2)$$
$$\boldsymbol{d}_1 = \frac{\ln\left(\frac{S_t}{K}\right) + \left(r + \frac{\sigma^2}{2}\right)}{\sigma\sqrt{t}} \qquad 45$$
$$\boldsymbol{d}_2 = \boldsymbol{d}_1 - \sigma\sqrt{t}$$

Also, the option chains were separated randomly into the training and testing parts, to evaluate the performance of the models on the unobserved data. The ratio for the training and testing parts were 70:30.

Number of individual options in each of the option chain can be seen in the Appendix 1, within the Option chains section. The implied coefficients were estimated under the risk-neutral probability measure. As all the underlying assets are denominated in the EUR currency, Euro area government zero coupon yield curve, published by the ECB, was used as the risk-free rate.

In the Tab.10 the performance of the models measured by the RMSE separately for the training and testing datasets can be seen. Where TRUE, the Variance Gamma model priced an option chain with lower RMSE. We are assuming that lower RMSE implies more precise fitting of the market option prices. Clearly, the VG model had lower error rate especially on the testing sample.

Table 10: RMSE of fitted models

RMSE - train			
		True	**False**
RMSE - test	**True**	26	3
	False	1	6

Data source: Eurex

5.3. Relation between the Moneyness and Relative pricing error

Finally, the relation between the root square relative pricing error and the Moneyness of the option was tested. The aim of this analysis was to test, whether the VG model can, at least partially, eliminate the Volatility smile effect. If the R^2 of the model would converge to zero, or the coefficients of the

Moneyness would be insignificant, the VG model would most likely be able to handle above mentioned problem. The Moneyness for each option is defined as

$$MN = \log\left(\frac{S}{K}\right) \quad \textbf{46}$$

and root square relative pricing error as

$$RSRPE_i = \sqrt{\left(\frac{C_i^{model} - C_i^{market}}{C_i^{market}}\right)^2} \quad \textbf{47}$$

For each option i in the above defined option chains and estimated implied coefficients from the previous chapter, the root square relative pricing error was calculated. Afterwards, for each option chain, the natural spline regression model (NS RM) was estimated in order to estimate the relationship between the MN and $RSRPE$.

As we expect that the relationship between the MN and $RSRPE$ will be similar for the option chains with the same maturity, Adj. R^2 from the separate NS RM was averaged for all the maturities and also for all the option chains, so the total comparison can be made. In the Tab.11 the average adjusted coefficients of determination of the fitted natural spline regression model with two degrees of freedom are reported. The significance of the Moneyness coefficients is not reported, as it was always significant on the 5 % confidence interval. The VG model pricing error was however less dependent on the moneyness than the BS model as the Adj. R^2 is in total average 19 % lower. For the option chains with yearly maturity, the Adj. R^2 difference between the models is even more significant. For these option chains, the difference in the average Adj. R^2 was more than 27% in total, favouring the VG model.

Table 11: R2 of the fitted models

	BS model	VG model	Difference
Adj. R^2 Total	76,2%	57,2%	-19,1%
Adj. R^2 Month	70,9%	57,6%	-13,3%
Adj. R^2 Half Year	72,8%	56,4%	-16,4%
Adj. R^2 Year	85,5%	57,6%	-27,9%

Tab. 12 shows the average RSRPE of the models, where the averaging is done with the same logic as in the previous table. The VG model was able to lower the RSRPE by 10 % in comparison with the BS model.

Table 12: RSRPE of the fitted models

	BS model	VG model	Difference
Total	30,11%	20,69%	-9,42%
Month	44,00%	37,61%	-6,38%
Half Year	28,59%	18,19%	-10,40%
Year	17,74%	6,26%	-11,49%

Figures 4 and 5 show the RSRPE (**Relative pricing error** axis in the graphs) of VG and BS models for the Henkel AG & Co. option chain, where all the options are maturing in a month time.

Figure 4: Henkel AG & Co. options pricing error of BS model

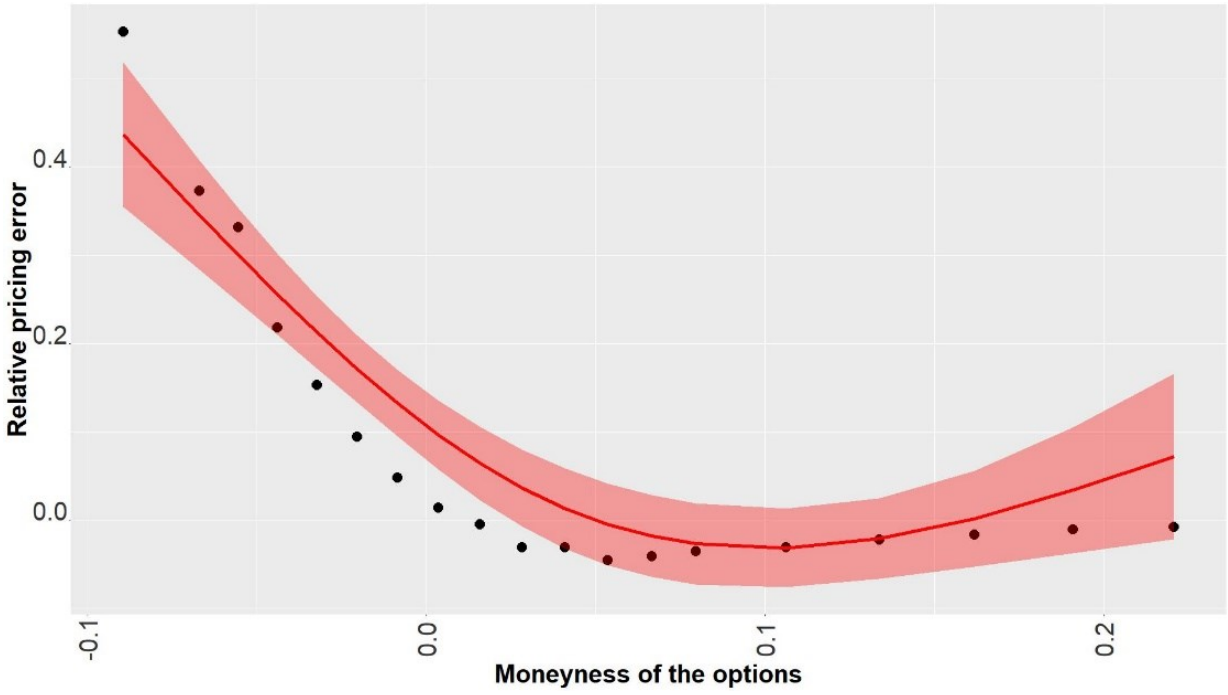

Figure 5: Henkel AG & Co. options pricing error of VG model

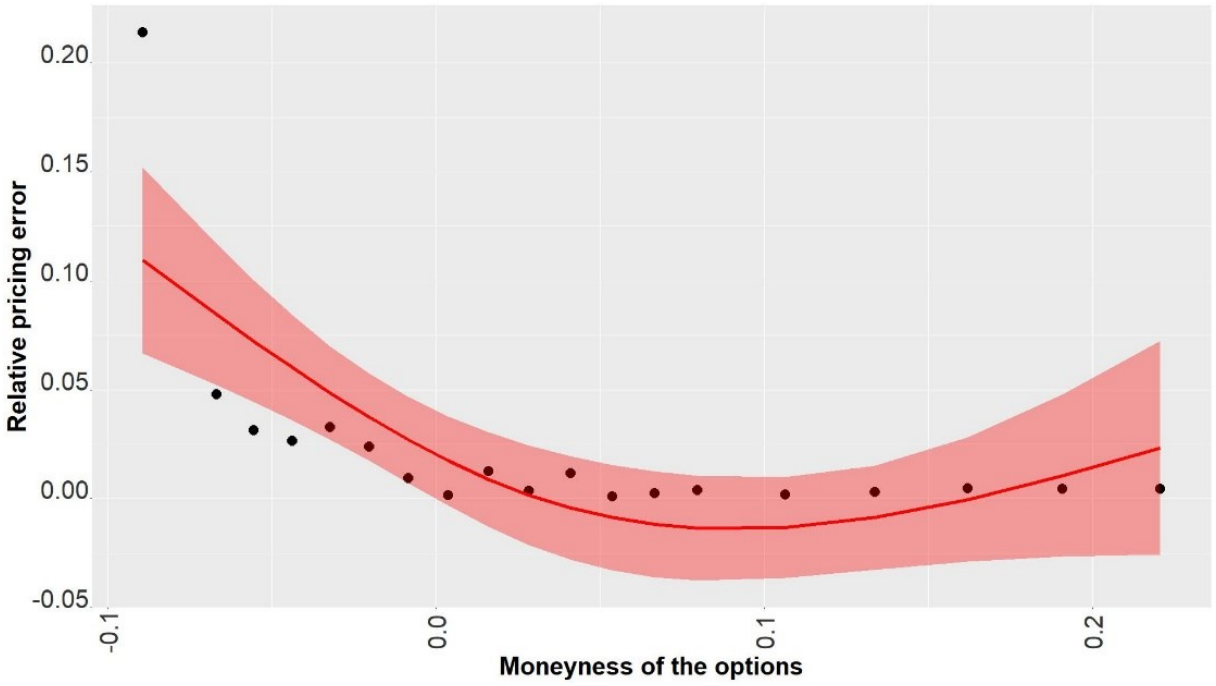

Figures 4 and 5 above illustrate, how the VG model was able to reduce the volatility smile phenomenon for the Henkel AG & Co. options with the one-month maturity. We can see that not only the variance of the RSRPE was reduced, but also that the fitted curve is flatter, and the errors are concentrated more around zero, below the 5 %, which can be considered as very accurate. Contrary to that, the BS

models pricing error surpass the 5 % level very often and the volatility smile effect can be clearly observed.

6. Conclusion

The aim of this paper was to propose appropriate solution of the Variance Gamma model for option pricing and compare the model with the Black-Scholes model.

Based on the analysis of the proposed algorithms, the Fast Fourier transformation algorithm is deemed to be the most efficient one, measured by the accuracy and computational efficiency.

Next, MLE method was used to fit Variance Gamma and Normal distributions to historical logarithmic returns with different frequency (daily, weekly, and monthly). This analysis proved the decreasing kurtosis assumption of the Variance Gamma. Also, the Variance Gamma distribution was preferred to Normal distribution, measured by the LL and BIC, in most cases.

The third analysis used both models to price the option chains and the RMSE metric was used to compare both models. Again, the Variance Gamma models was the preferred one.

Finally, both models were tested in relation to the Volatility smile phenomenon. The Variance Gamma model was able to reduce this phenomenon measured both by the Adj. R^2 and average root square relative pricing error.

As a result of the four performed analysis, the Variance Gamma model proved to be promising candidate, which can very precisely describe the leptokurtic financial distributions and partially eliminate the volatility smile effect phenomenon. On top of that, the Variance Gamma model does not require unrealistic assumptions as the Black-Scholes model and is more consistent with the financial theory.

7. References

APPLEBAUM, D. (2004). Lévy processes and stochastic calculus. New York: Cambridge University Press.

BATES, S. (1996). Jumps and Stochastic Volatility : Exchange Rate Processes Implicit in Deutsche Mark Options. The Review of Financial Studies Vol. 9, No., 69-107.

BEKELE, A. (2016). Cooley-Tukey FFT Algorithms.

Broyden-Fletcher-Goldfarb-Shanno (BFGS) algorithm. (2020, April 3.). Retrieved from RTMath: https://rtmath.net/help/html/9ba786fe-9b40-47fb-a64c-c3a492812581.htm

CAPASSO, V. a. (2005). An introduction to continuous-time stochastic processes: theory, models, and applications to finance, biology, and medicine. Boston: Birkhäuser: Modeling and simulation in science, engineering & technology.

CARR, P., & MADAN, D. B. (1999). Option valuation using the fast Fourier transform.

CONT, R. (2002). Empirical properties of asset returns: stylized facts and statistical issues. Quantitive Finance.

CONT, R., & TANKOV, P. (2004). Financial Modelling with Jump processes. New York, London, Washington: Chapman & Hallj crc financial mathematics series.

CONT, R., & VOLTCHKOVA, E. (2005). A Finite Difference Scheme for Option Pricing in Jump Diffusion and Exponential Lévy Models. Society for Industrial and Applied Mathematics Journal Volume 43(4), 1596–1626. (31 pages).

CONT, R., & VOLTCHKOVA, E. (2005). Integro-differential equations for option prices in exponential Lévy models. Finance Stochastics 9, 299–325.

FIORANI, F. (2009). Option Pricing Under the Variance Gamma Process. Saarbrücken: VDM Verlag Dr. Müller.

FU, M. C.-Y. (2007). Advances in Mathematical Finance. Boston, MA: Birkhäuser Boston: Applied and Numerical Harmonic Analysis.

GRADŠTEJN, I. S., RYŽIK, I. M., & JEFFREY, A. (2007). Table of integrals, series, and products. 7th ed. Boston: Academic Press.

KATZOURAKIS, N. (2014). An introduction to viscosity solutions for fully nonlinear PDE with applications to calculus of variations in L. New York: Springer.

KONIKOV, M., & MADAN, D. B. (2002). Option pricing using variance gamma markov chains. Review of Derivatives Research, 5(1), 81-115.

LÉVY, P. (1934). Sur les intégrales dont les éléments sont des variables. Pisa: Scuola Normale Superiore.

MADAN, D. B., CARR, P. P., & CHANG, E. C. (1998(2)). The Variance Gamma Process and Option Pricing. European Finance Review, 79-105.

MALKIN, C. (2019, December 29). Fast Fourier Transform. Retrieved from https://towardsdatascience.com/fast-fourier-transform-937926e591cb

MATHEWS, J. H., & Kurtis, K. (2004). Numerical Methods Using Matlab, 4th edition. ISBN: 0-13-065248-2.

MATSUDA, K. (2004). Introduction to Option Pricing with Fourier Transform. New York: Department of Economics, The Graduate Center, The City University of New York.

MILNE, F., & MADAN, D. (2008). Option pricing with V.G. martigale components. Kingston, Ontario, Canada: Department of Economics, Queen's University.

OSGOOD, B. (2007). The Fourier Transform and its Applications. Stanford University: Electrical Engineering Department.

SHEWCHUK, J. R. (1994). An Introduction to the Conjugate Gradient Method Without the Agonizing Pain. Pittsburgh: School of Computer Science Carnegie Mellon University.

SCHMELZLE, M. (2010). Option Pricing Formulae using Fourier Transform: Theory and Application.

SCHOUTENS, W. (2003). Lévy processes in finance: pricing financial derivatives. New York: J. Wiley.

TALEB, N. N. (2013). Fat tails and asymmetries: Risk and probability in the real world.

8. Appendix: List of companies

Historical returns

Source for the historical returns data is Yahoo Finance server.

Adidas
Daimler
JCDecaux SA
E.ON
Henkel AG & Co. KGaA
KBC Group NV
L'Oréal S.A.
Siemens Healthineers AG
Siemens Aktiengesellschaft
Strabag SE
Veolia Environnement S.A.

Option chains

Source for option chain data is Eurex server.

Option chains snapshot is 22nd October 2020. Each item in the table below represents one option chain.

Figure 6: Number of options in the option chain

Underlying asset	Number of options in the option chain		
	Monthly maturity	Half-year maturity	Yearly maturity
Adidas	35	17	9
Daimler	43	30	12
KBC Group NV	41	23	17
E.ON	30	13	10
JCDecaux SA	34	15	11
Deutsche Börse AG	35	17	10
L'Oréal S.A.	15	19	10
Strabag SE	18	16	10
Siemens Healthineers AG	18	15	9
Siemens Aktiengesellschaft	29	10	9
Veolia Environnement S.A.	39	18	17
Henkel AG & Co. KGaA	20	17	11

FFA Working Paper Series

2019

1. Milan Fičura: Forecasting Foreign Exchange Rate Movements with k-Nearest-Neighbor, Ridge Regression and Feed-Forward Neural Networks

2020

1. Jiří Witzany: Stressing of Migration Matrices for IFRS 9 and ICAAP Calculations
2. Matěj Maivald, Petr Teplý: The impact of low interest rates on banks' non-performing loans
3. Karel Janda, Binyi Zhang: The impact of renewable energy and technology innovation on Chinese carbon dioxide emissions
4. Jiří Witzany, Anastasiia Kozina: Recovery process optimization using survival regression

2021

1. Karel Janda, Oleg Kravtsov: Banking Supervision and Risk-Adjusted Performance in the Host Country Environment.
2. Jakub Drahokoupil: Variance Gamma process in the option pricing model.

All papers can be downloaded at: wp.ffu.vse.cz

Contact e-mail: ffawp@vse.cz

Faculty of Finance and Accounting, Prague University of Economics and Business, 2021

Winston Churchill Sq. 1938/4, CZ-13067 Prague 3, Czech Republic, ffu.vse.cz